Winter 12-1-2013

EMG-EMG Coherence Analysis of Elbow and Shoulder Muscles

Manu Stephen
Washington University in St. Louis

Washington University in St. Louis
School of Engineering and Applied Science
Department of Mechanical Engineering

Thesis Examination Committee:
Dr. David Peters
Dr. Guy Genin
Dr. Wilson Z. Ray

EMG-EMG Coherence Analysis on the Elbow and Shoulder Muscles

by

Manu Stephen

A thesis presented to the School of Engineering
of Washington University in partial fulfillment of the
requirements for the degree of

Master of Science

December 2013
Saint Louis, Missouri

ABSTRACT OF THE THESIS

EMG-EMG Coherence Analysis on the Elbow and Shoulder Muscles

by

Manu Stephen

Master of Science in Mechanical Engineering

Washington University in St. Louis, 2013

Motor coordination can be described by the activation of a few intermuscular coordination patterns, or muscle synergies. Muscle synergy can be defined as a relatively fixed pattern of activation across a set of muscles. The neural mechanisms underlying muscle synergies remain to be fairly unknown.

Through a muscle synergy study [13], co-activation in muscle pairs was discovered through a non-negative matrix factorization (NMF) analysis. In order to evaluate the same muscles under the frequency domain, coherence analysis (a correlational method) was used. Additionally, a comparison can be made to determine if the resulting muscle pairs overlap with the muscle pairs found through the synergy analysis.

Using coherence analysis, it was evaluated whether muscle members co-activated within a muscle synergy are correlated in the frequency domain, suggesting a common fixed drive in the central nervous system.

Acknowledgments

First and foremost, I would like to thank Dr. Peters. Without you, I would not have experienced the incredibly successful and driven atmosphere that Washington University provides. Your continual support, guidance, and willingness to help have opened a countless number of doors in helping me find my passion.

I would also like to thank Dr. Jinsook Roh, Dr. Zev Rymer, and the Sensory Motor Performance Program at the Rehabilitation Institute of Chicago. This research would not be possible without your direction, support, and drive to create a meaningful impact.

To my friends – this thesis would definitely have been possible sooner without you and your distractions. However, this would also require you all to be far less amazing than you are now. Thanks for the endless laughs, wonderful conversations, adoption of homeless dogs, and general debauchery – I wouldn't have it any other way.

Last but not least, to my family – thank you to the greatest role models I know. You are always there to push me to achieve my best and succeed, especially when I need it the most. Nothing would be possible without your unwavering support, care, and love. I couldn't ask for anything more.

Manu Stephen

Washington University in St. Louis
December 2013

Dedicated to my family and friends – near and far

Contents

List of Tables

List of Figures

Chapter 1

Introduction

Motor control has continually been involved in general daily tasks of any individual. The completion of such a task, such as lifting a cup, requires a complexity of movements that remain largely undefined. These seemingly effortless actions involve a large magnitude of motor units interacting within muscle fibers. In order to simplify these actions, a number of studies have been put forth on the interaction between the central nervous system (CNS) and motor units of the final product resulting in a movement. Some investigators claim that the CNS creates a hierarchical architecture broken down into specific building blocks that combine to create different movements [2]. To continue this postulation, further studies questioned if simple units can be flexibly combined in order to complete motor tasks [5]. This approach was addressed by simplifying motor tasks into specific modules, which can be defined as functional units in the spinal cord that correspond to a given motor output through utilizing a specific pattern of muscle activation [5] also known as muscle synergies.

In order to understand the significance of muscle synergies, it is important to question their formation. Since natural movements utilize a number of muscles, the construction of muscle synergies could be resultant of a common fixed drive or simply an occurrence of a specific motor coordination. Additionally, muscle

synergies can address the issue of the degrees of freedom in motor control – through using a smaller number of variables, the CNS can more effectively manage movements instead of controlling each motor unit individually [26].

This issue has been investigated thoroughly in a multitude of ways. Most commonly, studies collect electromyography (EMG) data to be analyzed, typically through correlational and computational methods. Upon completing the analysis, the EMGs are then inspected to see if certain muscle synergies exist and if these synergies are relevant to the task performed [26]. In terms of the statistical analysis, correlational and computational methods provide varying perspectives, potentially disadvantageous when used alone. For example, correlational methods alone may often confuse muscle relationships when different synergies are simultaneously recruited for a task. Furthermore, computational methods alone, such as non-negative matrix factorization (NMF) or independent component analysis (ICA), may focus on specific amplitude ratios, potentially overlooking general synergies occurring between groups of muscles. Therefore, the combination of combining NMF analyses with a correlational method, specifically coherence analyses, can account for these disadvantages, thus producing a more complete understanding of muscle synergies involved in a motor task. In this study, the EMG-EMG coherence of eight elbow and shoulder muscles was analyzed in conjunction with a NMF analysis of the same muscles.

1.1 Motivation

The motivation for this particular study has great implications for the field of neuromuscular diseases and orthopedics. Having a greater understanding of the underlying muscle activity and neural mechanisms could potentially be vital from reversing the effects of stroke to better designing prostheses for amputees. Through the use of electromyography (EMG), the electrical activity of muscles can be carefully analyzed to reveal muscle activation. This study specifically focused on surface EMG activity of the elbow and shoulder muscles.

1.2 Goal of Study

The goal of this study is to identify the muscles synergies in the elbow and shoulder muscles found through the non-negative matrix factorization (NMF) analysis, followed by replicating this 3-D isometric force task to undergo coherence analysis. Specifically, **Aim 1** is to define and identify the synergistic patterns through the completed NMF analysis. **Aim 2** is to replicate the task and perform coherence analysis to characterize upper limb muscle patterns during isometric force generation. To my knowledge, the study of coherence in conjunction with completed NMF analysis on the elbow and shoulder muscles during isometric force generation has not been previously studied with the techniques described.

1.3 Organization

This thesis is divided into three separate parts. The first part introduces the background to the study, electromyography, non-negative matrix factorization, coherence analysis, and current existing methodologies. The second part concentrates on the experimental design, methods, and implementation. The final part then focuses on the analysis and summary of results.

Chapter 2

Background

2.1 Electromyography

Electromyography (EMG) is a technique that measures the electrical activity during the contraction of muscles. A motor unit, which is defined as a motor neuron and the corresponding muscle fibers, will fire and cause an action potential to travel to from the neuron to the muscle. This electrical activity, known as a motor unit action potential (MUAP), is the result that appears from an EMG recording.

2.1.1 Neurophysiology

A given motor unit contains the corresponding muscle fibers being innervated, the axon's connection to the fibers, and the neuromuscular junction [3]. When the action potential travels down the axon and across the junction at a rate of approximately 4 m/sec, this potential stimulates the muscle fibers of the motor unit. Typically, the resting membrane potential of a skeletal muscle is around -95 mV. However, when the action potential reaches the axon terminal, vesicle release acetylcholine, causing the opening of sodium ion channels, which in turn causes the potential to reach the threshold voltage (-50 mV), allowing the action potential to travel down the muscle fiber [16]. Typically, motor units fire at a rate of 7-20 Hz, depending on the muscle.

However, an increase in firing frequency can occur if all motor units are recruited, potentially at a rate higher than 50 Hz [15].

2.1.2 Brief History

Experiments by Francesco Redi in the late 1600s first documented the discovery of electrical activity within the muscle of an electric eel. Nearly a century later, further work by Luigi Galvani confirmed that static electrical activity could in fact produce muscular contractions [8]. It was not until the mid-1800s that the invention of the galvanometer allowed for clearer evidence for the existence of an action potential in frog muscle. The early 1900s paved the way for scientists such as Pratt to confirm that the recruitment of muscle fibers, and not the size of the neural impulse, was responsible for muscle contraction. With the invention of the concentric needle electrode and advances in amplifiers the following decades, the EMG signals continued to become cleaner and clearer.

2.1.3 Current EMG Technology

There are two leading methods of electromyography records: invasive and non-invasive. The popular invasive method, intramuscular EMG, involves needle electrodes inserted through the skin and into the desired muscle tissue. Intramuscular EMG is more commonly used when deep muscle tissue or specific local muscle activity is being analyzed. Though this method provides high resolution of the signal, the invasive nature tends to be painful to the patient or subject and is therefore less preferred. The more popular non-invasive method,

surface EMG, uses an electrode on the surface of the skin to reveal underlying muscle activity. Though this may not provide information on specific muscle fibers, general muscle activation can be easily observed. Additionally, the non-invasiveness allows for greater comfort with patients and subjects, as well as ease of use in experiments. Surface EMG electrodes are commonly used in research labs, and are the type of electrodes used in this particular study.

Figure 2.1: Delsys Surface EMG electrode used in this particular study [4]

These surface electrodes can then be placed on the desired muscle/s for recording. Each electrode placed will record the electrical activity of that particular muscle, as well as the ground electrode, and send the recorded information to an amplifier. The schematic in Figure 2.2 shows the hypothetical placement of two electrodes, one on the bicep and the other on the triceps muscle.

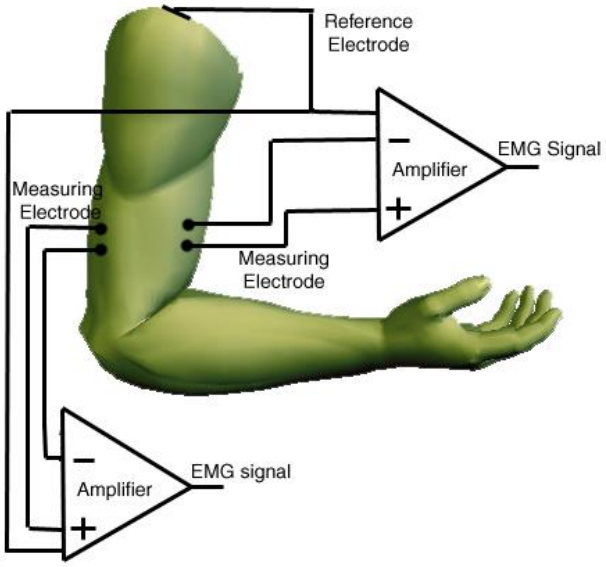

Figure 2.2 EMG Electrode Placement Schematic [28]

Differential amplifiers are used to amplify an EMG signal, so as to reduce or eliminate signal noise by subtracting the ground electrode signal from the muscle electrode. The amplifier takes the two inputs and amplifies the difference between them, producing a raw EMG signal, seen in Figure 2.3.

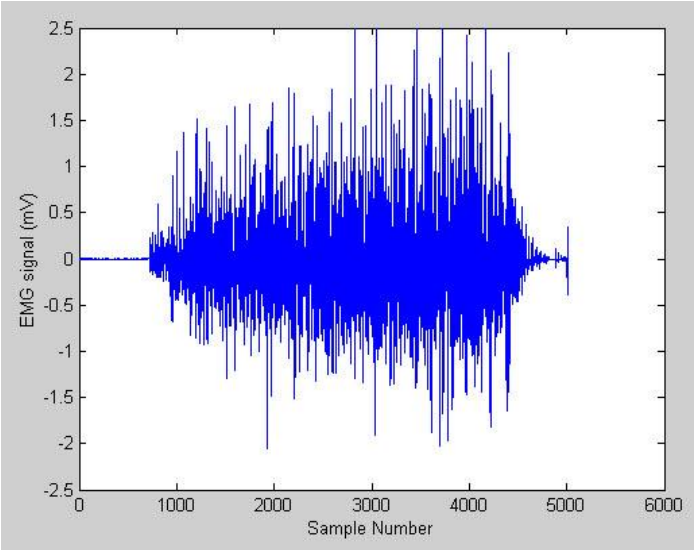

Figure 2.3 Sample Raw EMG Signal [28]

However, in order for this EMG to be properly processed and analyzed, it needs to undergo a full wave rectification, which removes negative values by taking the absolute value, and a low pass filter. The resulting rectified and low-pass filtered signal, seen in Figure 2.4, will be more useful for data analysis and further processing.

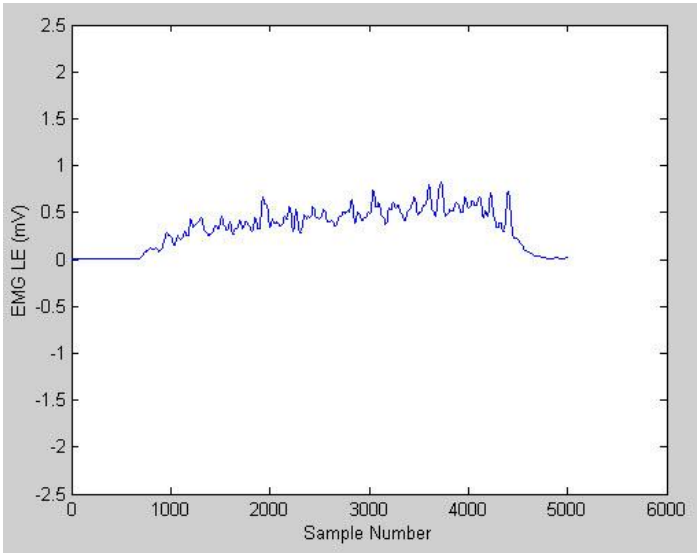

Figure 2.4 Sample Rectified and Low-Pass Filtered EMG Signal [28]

2.2 Non-negative Matrix Factorization

Non-negative matrix factorization (NMF) is an algorithmic approach in which a matrix is factorized into typically two matrices, with all three matrices containing no negative elements. The NMF method differs itself from other methods, such as principal component analysis, through its use of non-negativity constraints. These constraints allow the NMF method to a parts-based rather than holistic representation of a data set [18]. For example, the holistic approach of independent component analysis (ICA) may overlook complexities of parts that occur together. This prime difference is particularly useful when applied to EMG data as it will provide more physiologically translatable information. Once the EMG data is collected, it is processed according to the given task of the experiment and undergoes analysis for extraction of muscle synergies. This parts-based approach can be further understood by breaking down the EMG dataset into the mathematical form seen in Equation 1.

$$\mathrm{d(t)} = \sum_{a=1}^{N} c_a(\mathrm{t})\boldsymbol{w}_a \tag{1}$$

In Equation 1, d(t) represents a set of EMG data at a specific time point (t), with $c_a(t)$ as the time varying scalar coefficient for $\mathbf{w}_a$,and $\mathbf{w}_a$ representing the vector with regards to the *a*th synergy [7]. This can even be further simplified into a matrix notation shown in Equation 2.

$$D = SC \tag{2}$$

The simplified Equation 2 shows that the matrices “D” represents data, “S” corresponds to muscle synergies, and “C” to coefficient.

2.2.1 Novel NMF Approach

Previous studies have applied the NMF method to EMG signals in order to differentiate muscle synergies between tasks. One specific study [7] collected EMG signals from adult bullfrogs during unrestrained swimming and jumping experimental sessions in order to reveal underlying synergistic relationships. Upon pooling the datasets, a novel two stage synergy analysis was performed. The first stage involved extracting the different muscle synergies separately, which was completed through differentiating the synergies from the intact and deafferented data sets. The subspaces that the synergies spanned were then compared and assessed for commonalities. However, this analysis alone has some limitations - since a common subspace is not required to overlap or coincide with the subspace defined by a group of synergies, the extracted synergy from either dataset may not share that common subspace. In order to correct for this, the second stage of analysis involved a reformulation of the algorithm in Equation 1, using information from both intact and deafferented data sets simultaneously, allowing for shared synergies to be collected, which can be seen in Equation 3. The “in” and “de” superscripts stand for intact and deafferented, while the “sh”, “insp”, and “desp” mean synergies shared by two data sets, synergies specific to intact, and synergies specific to deafferented, respectively.

$$\mathbf{d}^{\text{in}}(t) = \sum_{a=1}^{N^{\text{sh}}} c_a^{\text{sh\_in}}(t)\mathbf{w}_a^{\text{sh}} + \sum_{a=1}^{N^{\text{insp}}} c_a^{\text{insp}}(t)\mathbf{w}_a^{\text{insp}};$$
$$\mathbf{d}^{\text{de}}(t) = \sum_{a=1}^{N^{\text{sh}}} c_a^{\text{sh\_de}}(t)\mathbf{w}_a^{\text{sh}} + \sum_{a=1}^{N^{\text{desp}}} c_a^{\text{desp}}(t)\mathbf{w}_a^{\text{desp}}, \quad (3)$$

Using the two stage analysis on 13 different muscles of the hind limb during jumping and swimming proved to be effective; shared and specific structures were found throughout multiple datasets, supporting the idea that a small number of muscle synergies activated by the CNS are integral to the generation of motor outputs.

2.2.2 NMF in Isometric Force Generation

In this specific study, the EMG data collected was through tasks performed under isometric conditions as linear combinations of a specific set of muscle synergies across eight different muscles [22]. This relationship is represented in Equation 4, characterized with the same form as Equations 1 and 2, with $W_{isometric}$ as an 8 X N matrix (N representing the number of muscle synergies), and $C_{isometric}$ as an N x T matrix (T representing number of trials).

$$EMG_{isometric} = W_{isometric} \cdot C_{isometric} \quad (4)$$

The EMG data was then pooled in order to evaluate for muscle synergies and analyzed in a similar two stage analysis as the study by Cheung, Bizzi (see Novel NMF Approach). The first stage extracted synergies separately from the dataset, which allowed for an estimate of the number of synergies necessary to reconstruct

the data. In the second stage, using the estimate from the first stage, the synergies were simultaneously extracted in shared and dataset specific synergies. In order to estimate the synergies from stage I, the variance-accounted-for (VAF) was calculated based on the entire dataset. This was defined as the trace of the covariance of the EMG data matrix, as shown in Equation 5, where SSE represents the sum of the squared residuals and SST is the sum of the squared EMG data.

$$VAF = 100 \text{ X } (1 - SSE/SST) \quad (5)$$

This calculation was repeated 100 times to characterize the distribution of the VAF and cross validate the values.

For this particular experiment, healthy subjects performed three different tasks: Spatial, Load, and Position. These tasks were all performed on a Multi-Axis Cartesian-based Arm Rehabilitation Machine (MACARM, further described in Chapter 3.1) in which subjects generate forces on a handle connected to a force transducer. Spatial tasks involved subjects generating voluntary forces in 210 different uniformly distributed directions in a 3D space with a load magnitude set to 40% maximum lateral force (MLF), which is the maximum amount of force that can be generated on the handle with the hand positioned in front of the shoulder at a distance of 60% of arm length. The load protocol involved the same generated movements but with force magnitudes at 10%, 25%, 40%, and 60% of MLF. The position protocol involved performing 3D force matches at eight force directions and

11 positions for a total of 88 target matches. The resulting muscle synergies following the two stage extraction and analysis can be seen in Figure 2.5.

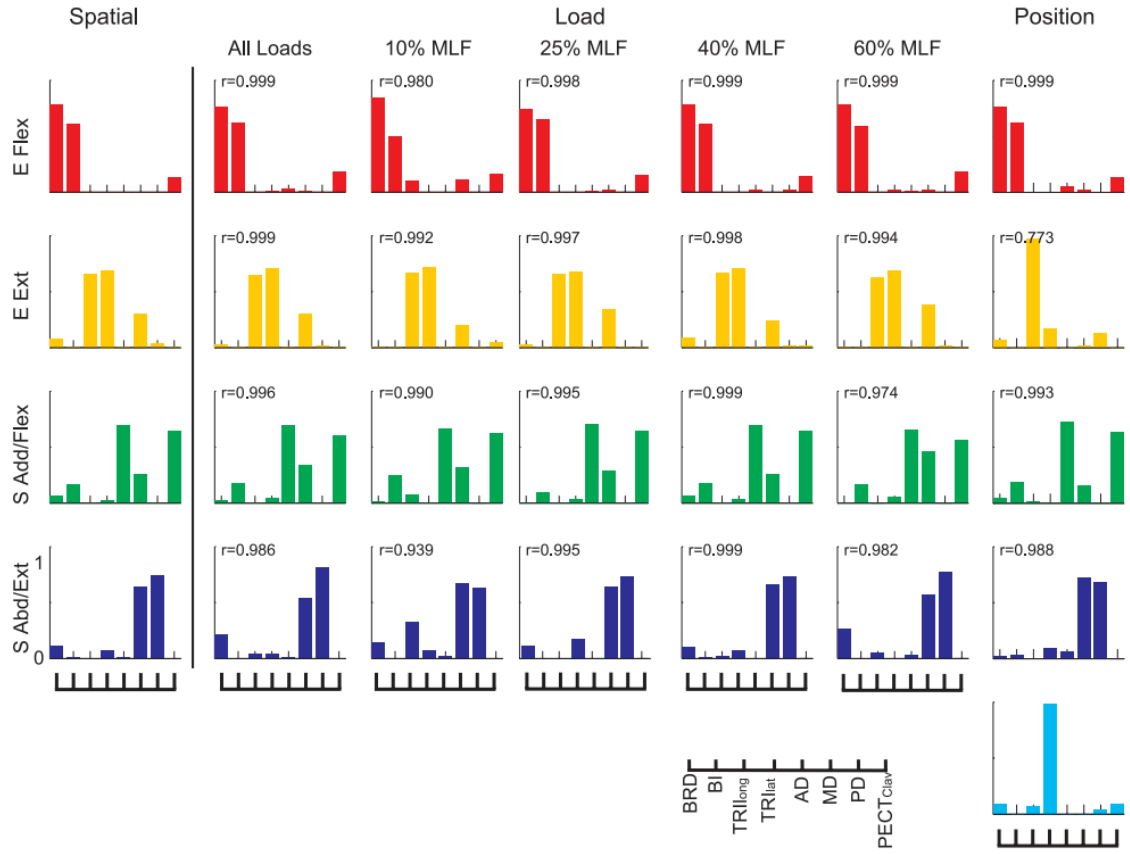

Figure 2.5 Muscle Synergies Underlying 3-D Force Generation [22]

The eight different muscles of the elbow and shoulder can be seen at the bottom right of Figure 1 and is as follows: brachioradialis (BRD); biceps brachii (BI); triceps brachii, long and lateral heads (TRIlong and TRIlat, respectively); deltoid anterior (AD), medial (MD), and posterior fibers (PD); and pectoralis major (clavicular fibers; PECTclav) [22]. From these muscles, there are four observed synergies:

elbow flexor (E Flex), elbow extensor (E Ext), shoulder adductor/flexor (S Add/Flex), and shoulder abductor/extensor (S Abd/Ext). Each synergy has a corresponding group of muscles that activate at significant levels together. For example, the elbow flexor synergy has strong activations from BRD and BI, as well as smaller activations from PECTclav. In the elbow extensor synergy, TRI long and TRI lat have strong concurrent activations, with MD activating at a lesser yet consistent magnitude. The shoulder adductor/flexor synergy has consistent activations from BI, AD, MD, and PECTclav, while shoulder abductor/extensor has the strongest activations with PD and PECTclav.

In this study, a coherence analysis on the same eight muscles was performed with healthy subjects at 40% of maximum voluntary contraction in the positive X direction. I hypothesize that the synergies discovered through the novel two stage NMF analyses will be in concurrence with the results found through coherence analysis.

2.3 Coherence

Coherence analysis was used to evaluate the relation of two sets of EMG data in the frequency domain. The coherence spectra is defined as the magnitude squared of the cross spectrum, normalized by the product of the auto spectra of the two individual data sets [8][14]. If there is a peak present in the cross power spectrum, there is a

common frequency that appears in both signals. However, this does not account for time as the frequencies could appear at separate points in time [1]. Thus, the coherence function computes the averaged estimates of the cross power spectrum and power spectra in segments. This method was first proposed by Welch [27], which is now known as the Welch method, and is used through the MATLAB function for this particular study.

The calculation for coherence is shown in Equation 6, where G_{xy} is the cross-spectral density between x and y, and G_{xx} and G_{yy} the autospectral density of x and y respectively.

$$C_{xy} = \frac{|G_{xy}|^2}{G_{xx}G_{yy}} \tag{6}$$

Coherence analysis provides a singular correlational value between 0 and 1, with 0 representing no correlation and 1 representing a perfect correlation. However, in real conditions, the coherence value is virtually guaranteed to result in less than 1 since the likelihood of two signals being identical at each point in time is incredibly low. Studies utilizing electrophysiological recordings (Electroencephalography (EEG), EMG, etc) have often taken advantage of coherence analysis in order to reveal relationships between muscle and muscle (EMG-EMG) or cortical activity and muscle (EEG-EMG). For studies that involve purely EMG recordings, coherence analysis can be used to understand the given coordination between a pair of muscles by looking at EMG signals in the frequency domain and identifying commonalities

in strength and periodicity of at relevant frequencies. Additionally, through analyzing the strength and frequency band distribution of the coherence spectrum, the common neural inputs to motor neuron pools can be revealed, which primarily originate from the corticospinal pathway (Danna-Dos Santos 2010). Some studies have also suggested that coherent oscillations in the motor system may direct activation of multiple muscles through mutual input from neuronal groups, creating a mechanism of efficient and effective interaction [25]

2.3.1 Relevant Coherence Studies

Current literature has shown a vast range of studies involving coherence analysis with electrophysiological recordings. Coherence has been especially used in the relation between cortical activity and muscle activation (EEG-EMG) recordings. This specific coherence, also called corticomuscular coherence (CMC), can be beneficial for revealing underlying cortical and muscular relationships following a neurological disorder, such as stroke.

One particular study assessed the cortical control of EMG activity through weak tonic contraction tasks such as elbow flexion, wrist extension, and power grip using all digits [19]. This study involved subjects performing tasks at a force level of 10-20% of the maximum force. The EEG signals were recorded through a 56 electrode cap while surface EMG recordings were taken from the right and left biceps muscle, right and left flexor carpi radialis muscle, and right and left opponens pollicis and first dorsal interosseous muscles (both located in the hand). Once the signals were

recorded, the data was segmented into 1024 ms epochs without overlap. The coherence was calculated through a reformulation of Equation 6, which can be seen in Equation 7.

$$|R_{xy}(i)|^2 = \frac{|f_{xy}(i)|^2}{f_{xx}(i) \times f_{yy}(i)} \quad (7)$$

In this equation, fxx(i) and fyy(i) represent autospectra of the EMG and EEG signals for a specific frequency (i). Fxy(i) represents the cross spectrum between the two signals. The output of this is the coherence value between 0 and 1. This study considered any coherence values significant when it was greater than 95% confidence limits, which was calculated from the number of epochs.

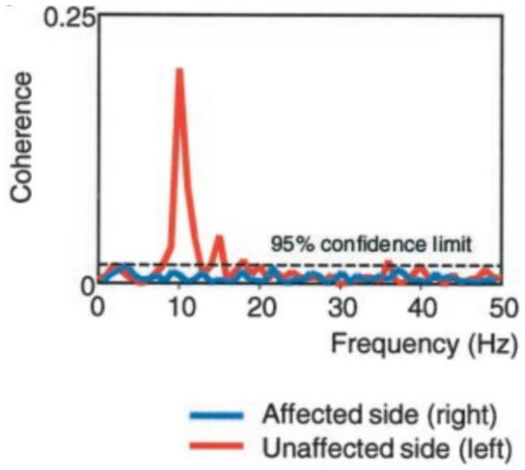

Figure 2.6 EEG-EMG Coherence Spectra [19]

The resulting EEG-EMG coherence spectra can be seen in Figure 2.6, with each spectrum in the same stroke survivor patient, thus the affected side vs unaffected side of the stroke. The frequency range of 3-50Hz is sufficient to cover the EEG power

spectra, and a peak can be seen at approximately 10 Hz on the unaffected side, which corresponds to motor unit activity.

There have also been a number of studies that have examined EMG-EMG coherence, which is further relevant to the present study, specifically regarding hand muscles during digit grasping. One study involved subjects using their thumb, index, and middle fingers to exert normal forces on a grip manipulandum at maximum voluntary contraction (MVC) and levels below MVC (sub MVC), specifically at 5%, 20%, 40%, 60%, and 80% of MVC (Poston 2010). These forces were to be generated as a sum total isometric force throughout the tasks. Similar to the EEG-EMG study, once the EMG signals were collected from six intrinsic and six extrinsic hand muscles, the frequency domain was analyzed for coherence. Each muscle had signals which were concatenated into 36,000 data points to create a long trial, in order to increase the number of disjoint sections, which in turn increases the reliability of the coherence values estimated (Maris et al 2007 – nonparametric statistical testing of coherence differences).

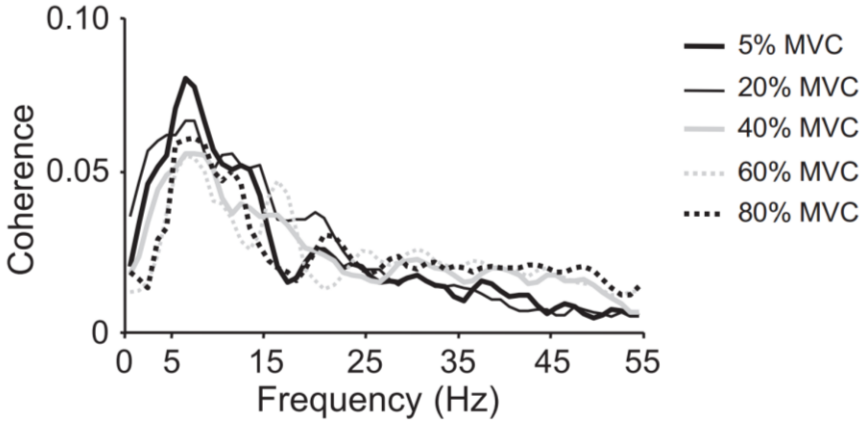

Figure 2.7 EMG-EMG Coherence Spectra at each %MVC (Poston 2010)

The resulting EMG-EMG Coherence can be observed in Figure 2.7 for each different percentage of MVC. The most significant peaks result between 5 and 15 Hz, which is common across multiple studies, reporting peaks between 1 to 12 Hz.

One study that observed EMG-EMG coherence between adults and children during a reaching and holding task reported significant coherence between 1 and 10 Hz with low a proportion of results showing coherence at frequencies above 10 Hz. It is also suggested in this study that the significant EMG-EMG coherences result from the synchronous oscillatory drive to motoneurone pools [7]. Lower frequency ranges, especially below 50 Hz, have been supported in a number of recent studies.

Publication	Goal/Methods	Coherence Range (x-axis) (Hz)	Coherence Range (y-axis) (Hz)
Patterns of EMG–EMG Coherence in Limb Dystonia - Grosse et al	EMG recordings taken from tibialis anterior of symptomatic and asymptomatic patients with dystonia	0-50 Hz, peak at 5-10 Hz	0-1, peak at 0.8/0.9
Influence of Fatigue on Hand Muscle Coordination and EMG-EMG Coherence During Three-Digit Grasping - Danna-Dos Santos et al	EMG-EMG Coherence taken from 12 hand muscles in finger contraction task	0-55 Hz, peak at 5-15 Hz	0-0.1, peaks at 0.05 and 0.1
Weakening of Synergist Muscle Coupling During Reaching Movement in Stroke Patients - Katarzyna Kisiel-Sajewicz et al	Surface EMGs recorded from stroke and healthy patients; Coherence observed in reaching muscles	"EMGs of the 2 synergist muscles was significantly higher in both the reaching and holding phases in the frequency range of 0 to 11 Hz"	0-0.5
Motor Unit Synchronization Is Increased in Biceps Brachii After Exercise-Induced Damage to Elbow Flexor Muscles - Dartnall et al	EMGs obtained during isometric contraction of elbow flexors; motor unit coherence analyzed	0-30 Hz, peaks at 1-10 Hz, smaller at 10 - 30 Hz	0-0.08
Neural Mechanisms of Intermuscular Coherence: Implications for the Rectification of Surface Electromyography - Boonstra et al	Surface EMGs taken from three ankle plantar flexion/extensor muscles during a standing task	0-60 Hz, peaks at 5-15 Hz	0-0.6
Changes in EMG Coherence Between Long and Short Thumb Abductor Muscles During Human Development - Farmer et al	EMGs recorded from short and long thumb muscles; 10-20% MVC	0-90 Hz, peaks between 5-40 Hz, especially around 20 Hz	0-0.2

Table 2.1 EMG-EMG Coherence Ranges in Recent Studies

This present study used similar methods to calculate EMG-EMG coherence across the eight different muscles in the elbow and shoulder. My hypothesis was that the coherence values will result in a similar frequency range and will suggest parallel muscle synergy groups as found through the NMF application.

Chapter 3

Experimental Design

Using a MACARM Robot and surface EMGs on 8 muscles of the upper limb, an isometric force generation task was performed on two right hand dominant healthy male subjects with no neurological, muscular, or orthopedic impairments.

3.1 MACARM Robot and EMG Placement

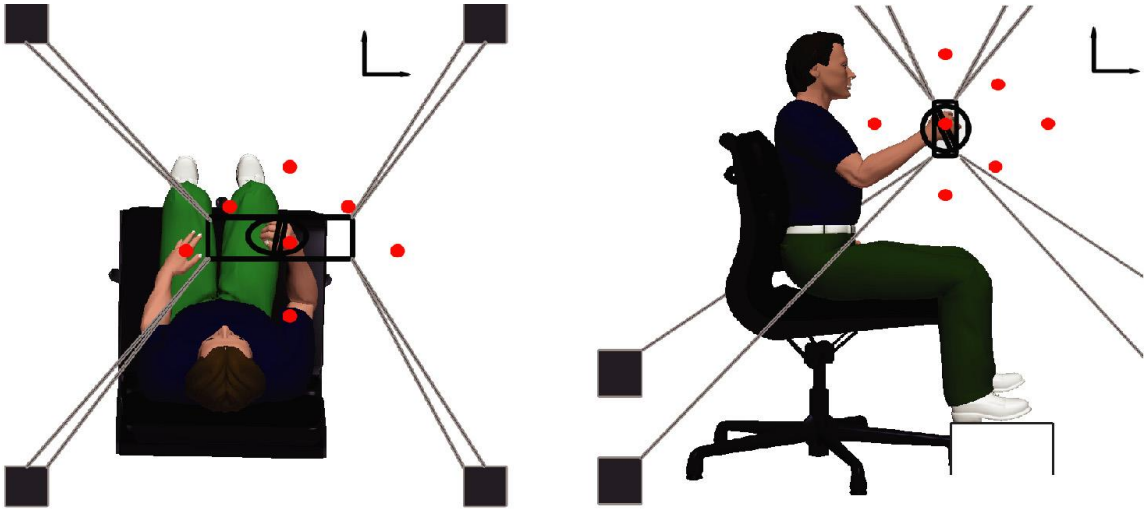

Figure 3.1: MACARM Robot Setup [13]

Hand position and 3-D forces generated were recorded using the Multi-Axis Cartesian-based Arm Rehabilitation Machine (MACARM; see Fig.3.1). The MACARM is a cable-based robot comprised of a spatial array of eight motors, connected via cables (Fig. 3.1) to a centrally located gimbaled handle (a rotating bar

in the middle of an oval around the subject's right hand; see Fig. 3.1), mounted on a six-degree-of freedom (DOF) load cell (Model #45E15A, JR3, Woodland, CA). Due to the amount of workspace available, the variance of positions was maximized, thus in turn maximizing EMG variance.

Surface EMG's were recorded from 8 muscles at the following locations: brachioradialis (BRD); biceps brachii (BI); triceps brachii, long and lateral heads (TRIlong and TRIlat, respectively); deltoid anterior (AD), medial (MD), and posterior fibers (PD); and pectoralis major (clavicular fibers; PECTclav) [13]. Additionally, an electrode was placed near the elbow as a ground or reference.

Electrodes were placed in accordance with the guidelines of the Surface Electromyography for the Non-Invasive Assessment of Muscles–European Community Project [11] [15]. Maximum voluntary contractions (MVCs) were performed prior to data collection to verify correct electrode placement. EMG signals were amplified (x 1000), band-pass filtered (20–450 Hz), and sampled at 1,920 Hz. Data acquisition was synchronized between the MACARM and EMG data acquisition computers through the use of a common clock and trigger.

3.2 Experimental Protocol

The task involved an isometric force generation, with subjects voluntarily generating this force under 54 different directions, uniformly distributed in 3-D space, with their

limb positioned in the middle of the workspace. The subject, seated in the middle of the workspace as shown in Figure 3.1, was first prepped by having eight EMG electrodes placed on the specified muscles (see Section 3.1) and one ground electrode on the elbow. In order to provide visual feedback of the force exerted, subjects were seated facing a LCD monitor display. Figure 3.2 shows an example of what is shown on a display: a target matching task required to be completed by the subject, in which the gray sphere must completely cover the stationary aquamarine sphere for approximately 45 seconds, both spheres identical in size. The different placements of the aquamarine sphere generated the 54 different uniformly distributed directions, requiring the subject to understand the depth perception of each placement. In the case of Figure 3.2, the sphere must be moved with an adequate amount of force, or load magnitude, in the negative x, positive y, and positive z direction.

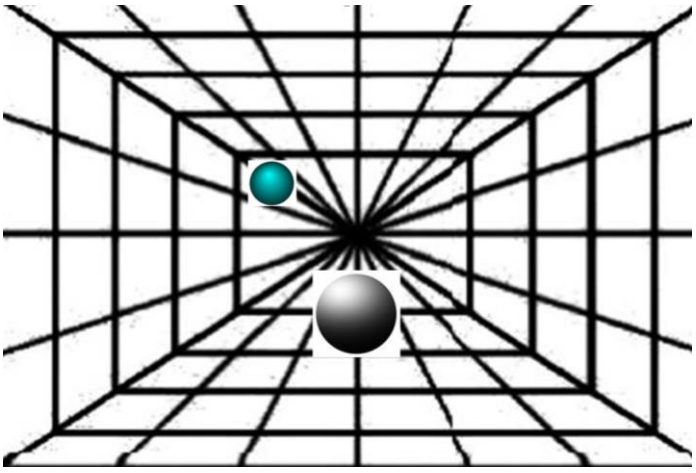

Figure 3.2 Target Matching Task in 3D Space

The display can be represented as a coordinate of ([1,-1], [1,-1], [1,-1]), which represents the location of the aquamarine sphere. For example, a coordinate for

Figure 3.2 could be (-0.4875, 0.8443, 0.2225). The 54 locations of the stationary sphere are represented by the red circles in Figure 3.3.

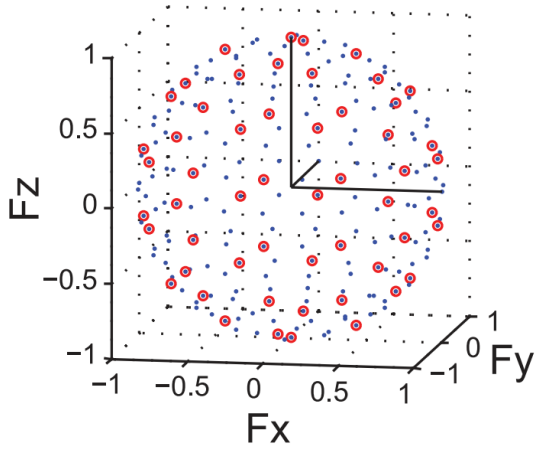

Figure 3.3 54 Target Force Directions in 3D Space

Before starting the task, the subject performed a number of unrecorded trials to familiarize with the MACARM and become comfortable with the target reaching task. In order to determine the load magnitude to set for each trial, the subject performed a series of maximum voluntary contractions. The subject would exert maximum force in the positive and negative X, Y, and Z directions through the visual display. The load magnitude was set at 40% of MVC (maximum voluntary contraction) in the positive X direction (see Figure 3.3) as that was determined to be the weakest direction in order to reduce chances of muscle fatigue. Studies typically use 10-20% of MVC, [7] [9], but since the weakest direction is being used, 40% will be enough to reduce fatigue.

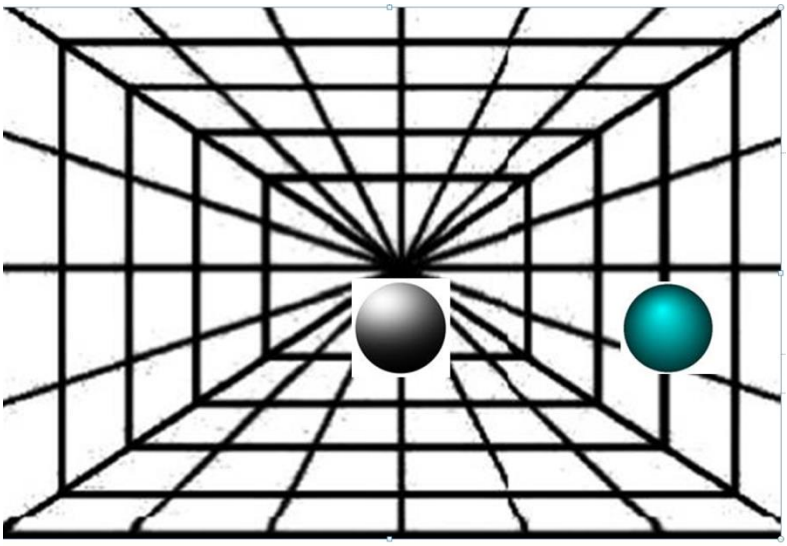

Figure 3.4 Positive X Direction Task to Calculate MVC

For each of the 54 positions in 3D space, three attempts were given to obtain a successful target match. Subjects had 9 seconds, including a 2 second baseline, to achieve a target match at a self-pace. EMG signals were recorded for a total of 60 seconds per direction, with force maintained for a minimum of 45 seconds, as the gray sphere encompassed the aquamarine sphere. This large amount of time for data collection is useful in increasing the number of datasets which will increase reliability, as previous studies have shown. Additionally, Welch's study has shown that a greater number of segments will provide more accurate results, assist in achieving a desired variance, and testing/measuring nonstationarity [16]. For healthy control subjects, this amount of time will be attainable. However, for stroke survivors, even with mild impairment, the collection time per direction will have to be decreased. Since stroke subject datasets will be shorter, overlapping segments will be necessary. Regardless of control or stroke patient, it should be noted that

between each trial, a 15-30 second break should be taken, again to reduce chances of muscle fatigue.

3.2 EMG Processing

After each trial during the task, the computer would display the EMG signals of each muscle, which allowed for visual inspection during the experiment to verify the absence of any artifacts or recording errors. The raw EMG signals were preprocessed as described in Section 2.1.3, through rectification and band pass filtering (20-450 Hz). The data for each muscle was concatenated across trials, creating a large data set for each of the eight muscles containing 96,000 data points. As found in earlier studies, this longer data set allows for creating a larger amount of segments, which in turn allow for increased reliability with the coherence values.

The coherence was calculated in accordance with a number of previous studies, following the formula as described in Equation 7, as well as using Welch's periodogram. In this method, a discrete window function $w = (w_0, \ldots, w_{Ne-1})$ is applied to each signal epoch $x^{(j)}$ with the length N_e. This periodogram is obtained through Equation 8, in which M_e is the overlapping number of epochs and U is the window energy.

$$P_x(f_k) = \frac{1}{M_e} \sum_{j=1}^{M_e} \left(\frac{1}{N_e f_s U} \left| \sum_{n=0}^{N_e-1} w_n x_n^{(j)} e^{-i2\pi nk/N_e} \right|^2 \right) \quad (8)$$

With the assistance of MATLAB's built in functions, Welch's periodogram method with a Hamming window of 1920 sample length was used, with overlapping segments of 960 sample length in order to increase the number of data segments. An original code was written to properly analyze the data and present results accordingly, as seen in Appendix B.

Previous EMG coherence studies have also used similar Hamming window with half sample length overlap [6]. The analysis was conducted between each pair of muscles for each direction, resulting in 28 different coherence plots per target direction. However, plots were created according to muscle pair, and so including repeat plots, a total of 64 plots were produced (8 per muscle; Appendix A) for each of the 54 target directions. This allowed for easier comparison to focus on one individual muscle's coherence in relation to others.

For the statistical analysis portion, a z-transform and a 95% confidence interval should be conducted on the dataset of coherence values. Various studies perform the z-transform [14][9][12] to normalize the dataset through the arc hyperbolic tangent transformation, as shown in Equation (8),which is particularly useful with pooled coherences.

$$z = \frac{1}{2} \ln \frac{1+r}{1-r} = \operatorname{artanh}(r) \tag{9}$$

Pooled coherences are similar to individual coherences in that it provides a normative measure of linear association between 0 and 1 [7]. In order to calculate pooled coherence, the individual coherence estimates are combined. The pooled coherence at frequency (λ) across *k* records is shown in Equation 10.

$$\left| \frac{\sum_{i=1}^{k} L_i R_{xy}^{i}(\lambda)}{\sum_{i=1}^{k} L_i} \right|^2 \tag{10}$$

In this equation, R^{i}_{xy} (λ) represents the individual coherence for record *i*, which has been calculated from L_i segments of data. The pooled coherence provides a value which describes the correlational structure amongst a population. The significance of pooled coherence values rely on the subject population, since any inferences from the value relate to the population as a whole. For this particular study, since the subject population involved is so low, the pooled coherence was not found to be useful or relevant.

Statistical significance for individual coherence was computed through the mean, critical value, and standard deviation for each coherence analysis to compute the 95% confidence interval per muscle pair, as shown in Equation (11).

$$\overline{x} \pm z\frac{s}{\sqrt{n}} \tag{11}$$

Previous studies also found a larger number of datasets to be important in order to calculate 95% confidence intervals for EMG-EMG coherence accurately [7]. The

resulting graphs have a horizontal line accounting for the upper 95% confidence limit based on the assumption of independence.

Chapter 4

Overall Analysis

4.1 Results

I believe the data show some similarities in muscle synergies between the NMF applied method and the EMG-EMG coherence of the same muscles in this isometric force generation experiment. Through visual inspection, higher magnitudes of coherence can be observed in the frequency range of 0-50 Hz.

During each of the 54 trials, raw EMG signals are recorded through the amplifier and are displayed on the computer. In order to process the data for coherence analysis, the signal must be rectified and low pass filtered. Figure 4.1 shows an example of rectified EMG signals compiled throughout all of the trials on the BRD (brachioradialis) muscle.

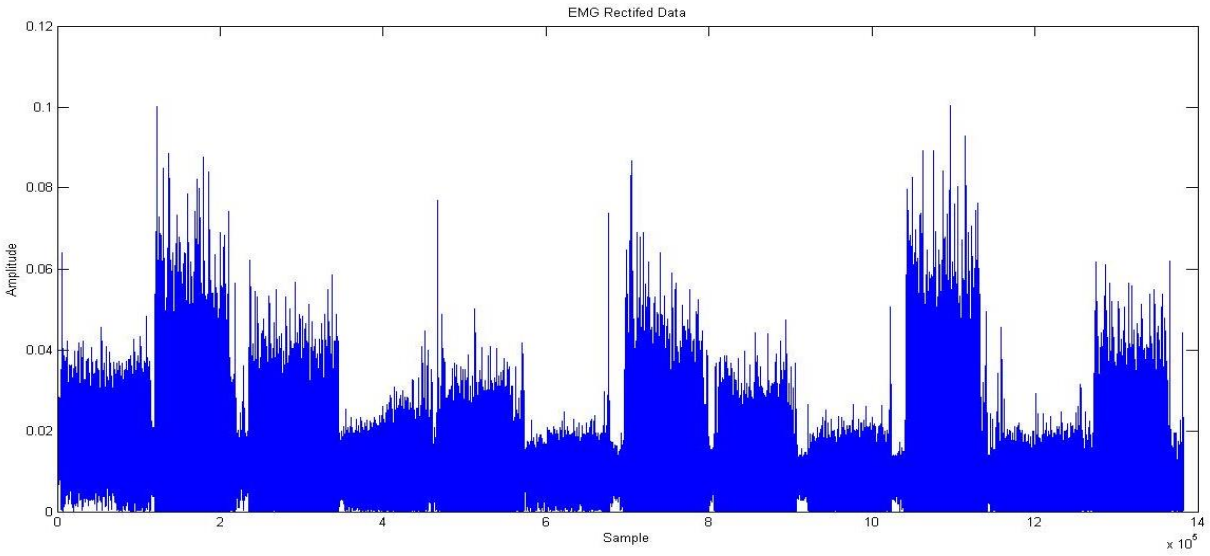

Figure 4.1 Rectified Data of BRD Muscle throughout Trials

Additionally, a Fourier transform was performed on each muscle throughout trials to visually inspect the frequency response for the task, which is shown on Figure 4.2.

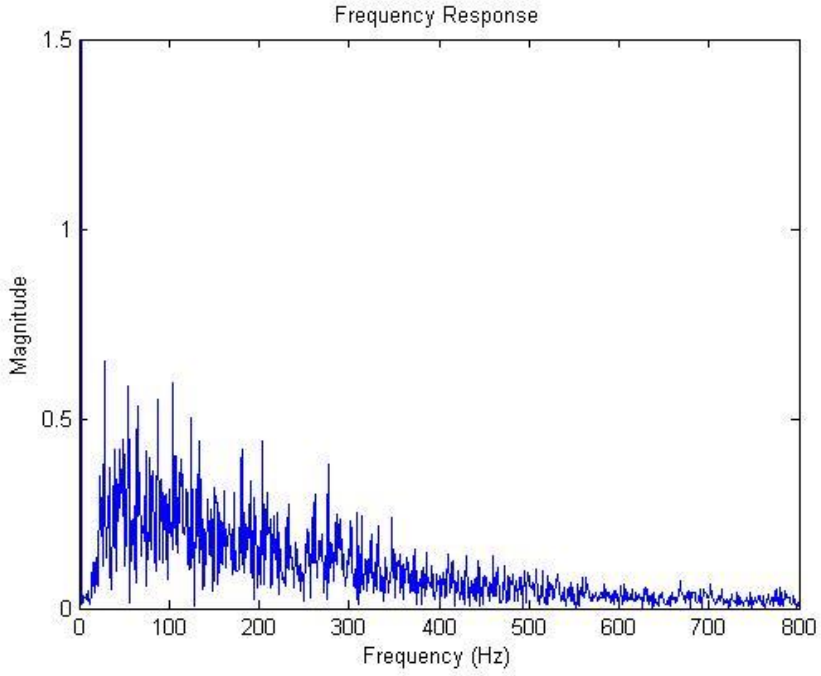

Figure 4.2 Fourier Transform of BRD Muscle throughout Trials

It can be observed that the higher amplitude of frequencies occur in the lower range of frequencies. This is concurrent with studies suggesting that lower frequencies correspond to motoneuronal drives relevant to the task. However, in order to further analyze this, the frequencies were analyzed on a smaller scale between muscles for coherence.

In order to evaluate the findings, the coherence was computed for each of the eight muscles across 54 trials. With the analysis being performed both for individual trials as well as across trials, coherence values can be observed for both trial-specific and

muscle-specific throughout task scenarios. When plotting the coherence values, a graph was created for each muscle paired against itself and the other muscles. These graphs can be seen in the following Figures 4.3 through 4.10.

BRD vs. All

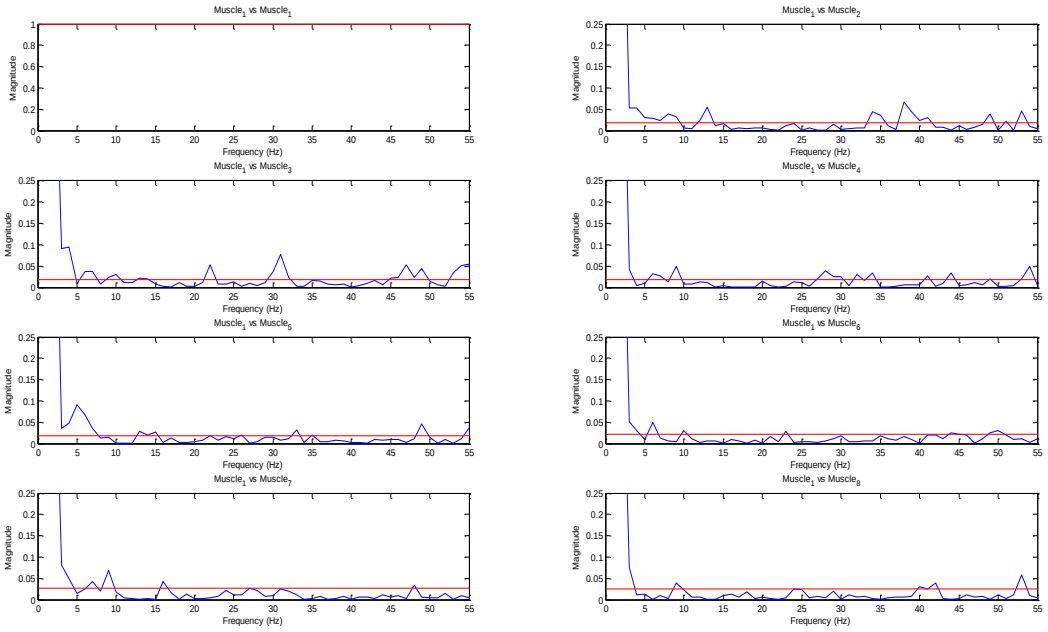

Figure 4.3: Target 1, Coherence of BRD vs. All

BI vs. All

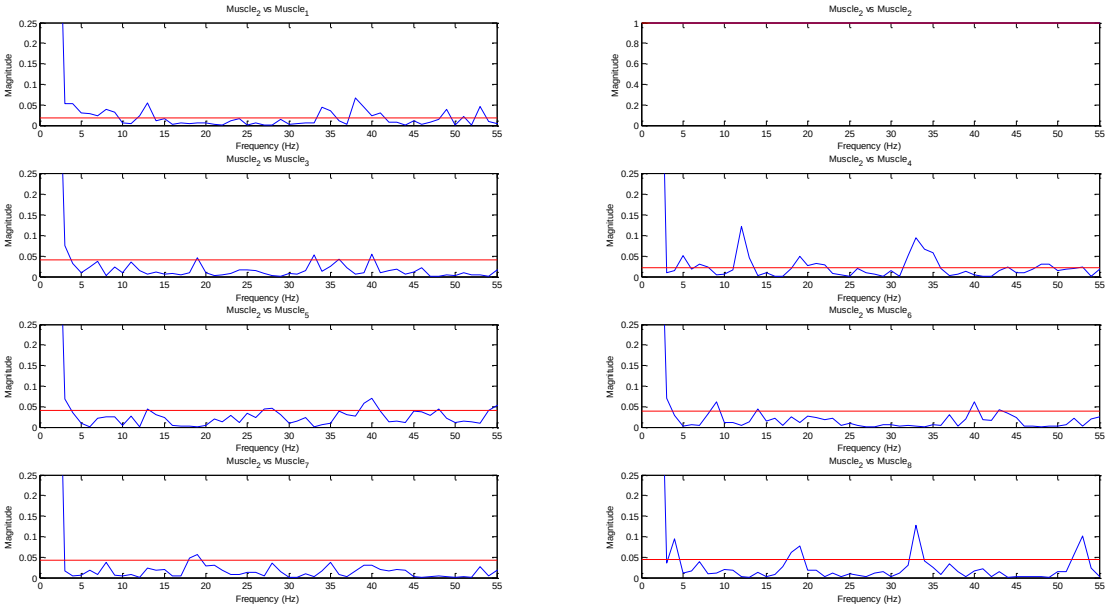

Figure 4.4: Target 1, Coherence of BI vs. All

TRIlong vs. All

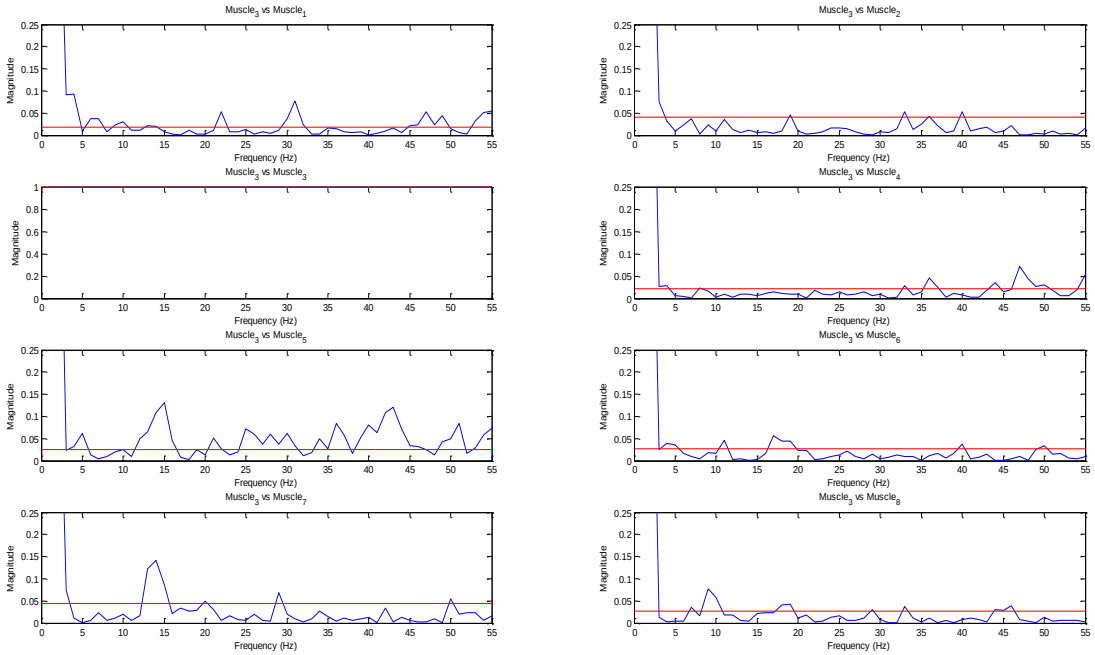

Figure 4.5: Target 1, Coherence of TRIlong vs. All

TRIlat vs. All

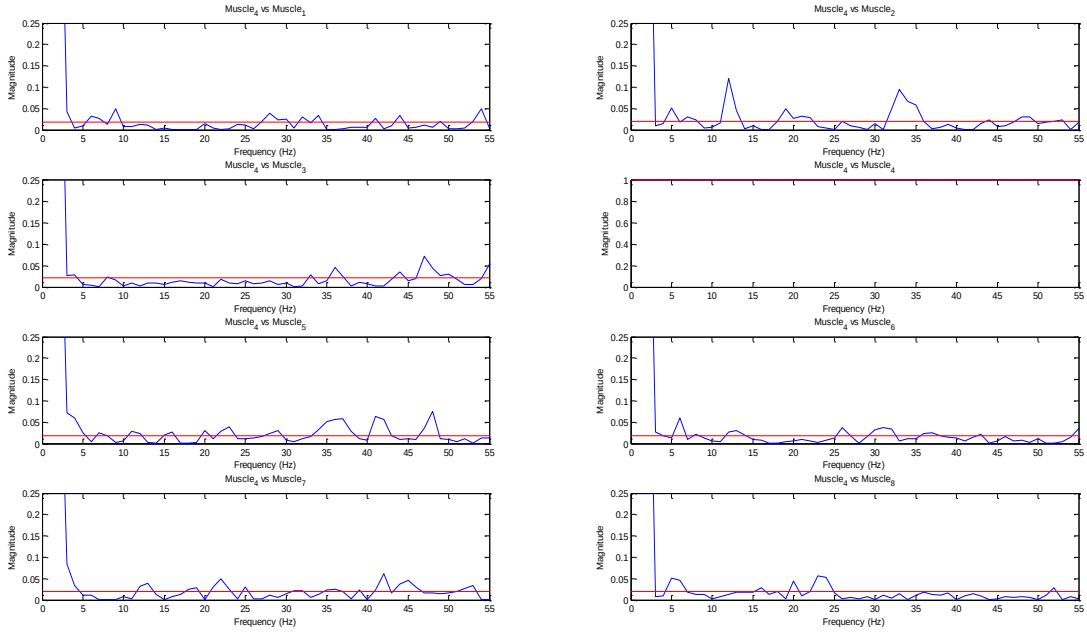

Figure 4.6: Target 1, Coherence of TRIlat vs. All

AD vs. All

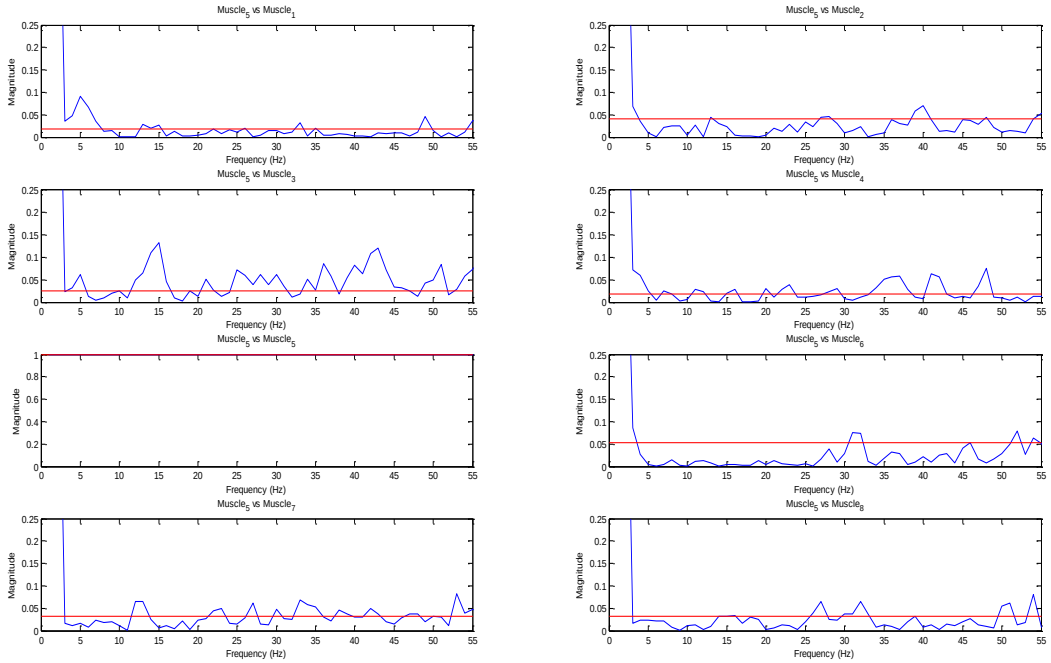

Figure 4.7: Target 1, Coherence of AD vs. All

MD vs. All

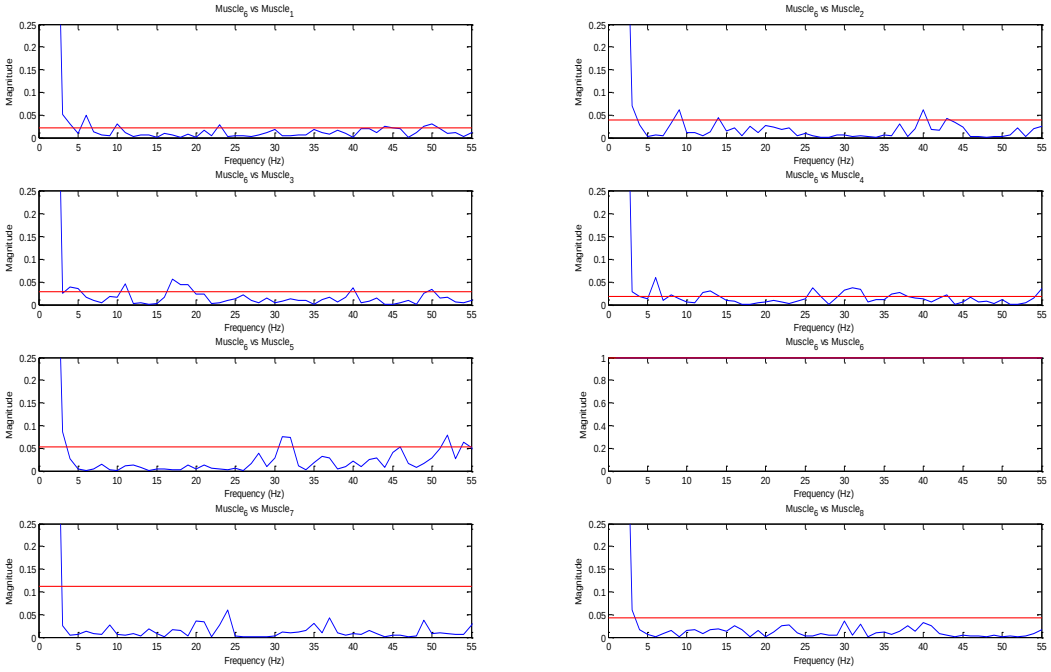

Figure 4.8: Target 1, Coherence of MD vs. All

PD vs. All

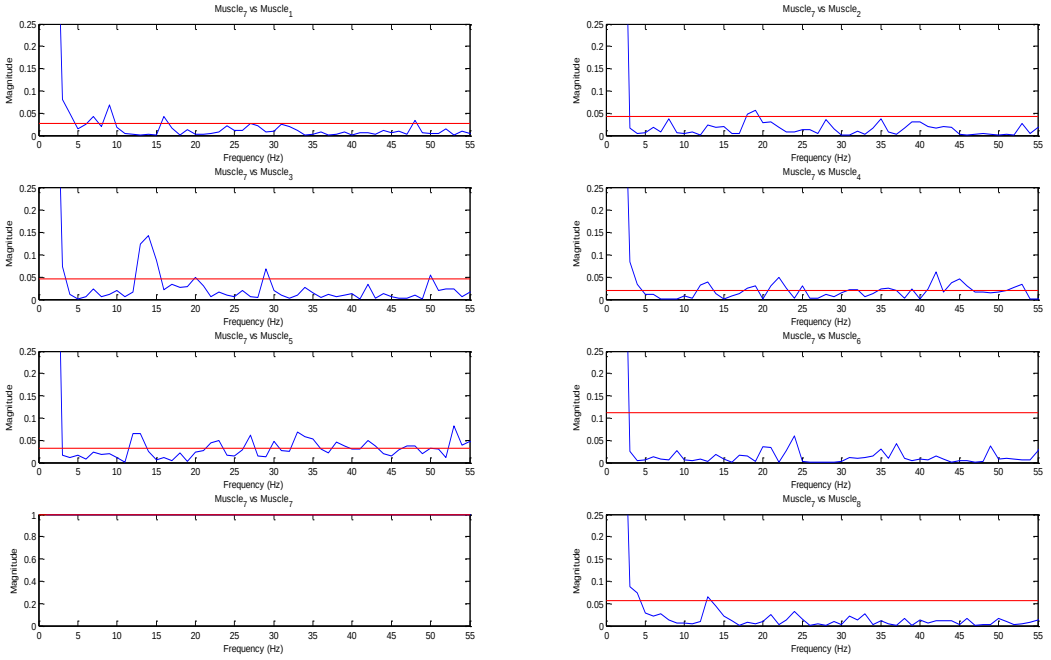

Figure 4.9: Target 1, Coherence of PD vs. All

PECTclav vs. All

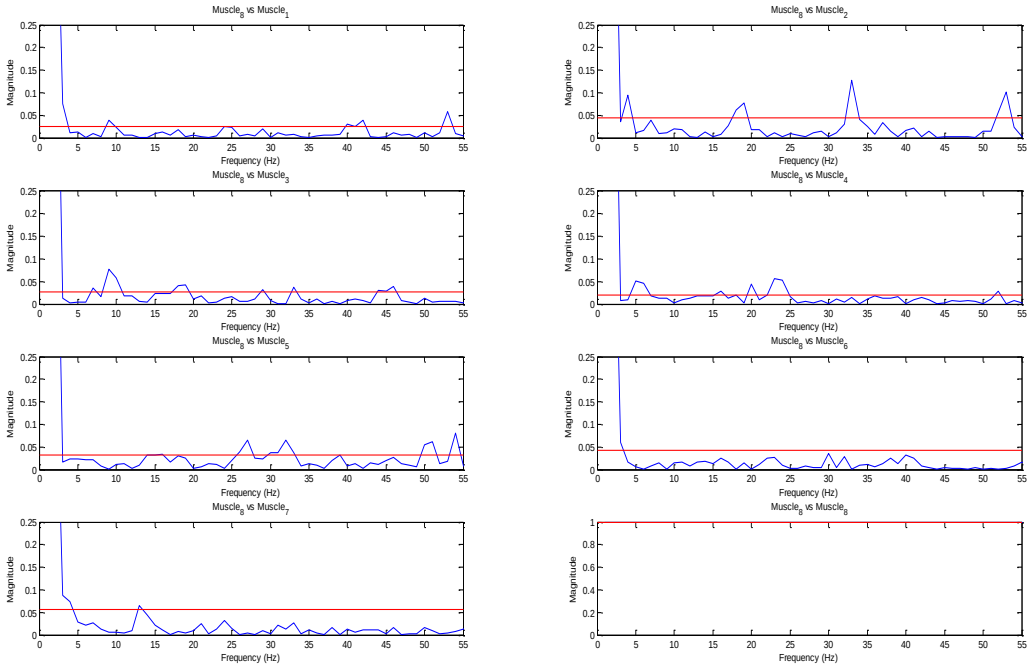

Figure 4.10: Target 1, Coherence of PECTclav vs. All

These figures represent the coherence values for each muscle against the other for Target 1, in which the sphere is placed in the negative X, Y, and Z coordinates (-0.7436, -0.2416, -0.6235). In each figure, there is one graph that which seems blank and contains a horizontal line at 1. This represents the coherence dataset paired against its self, and this result is expected since the two signals are identical. This was intentionally included as a corrective measure to ensure that each graph compared the correct signals of data. These graphs only represent the data for Target 1, shown as an example – the entirety of the data incorporates this method for each

target and each muscle, resulting in 8 graphs per target, or a total of 432 graphs for the full task.

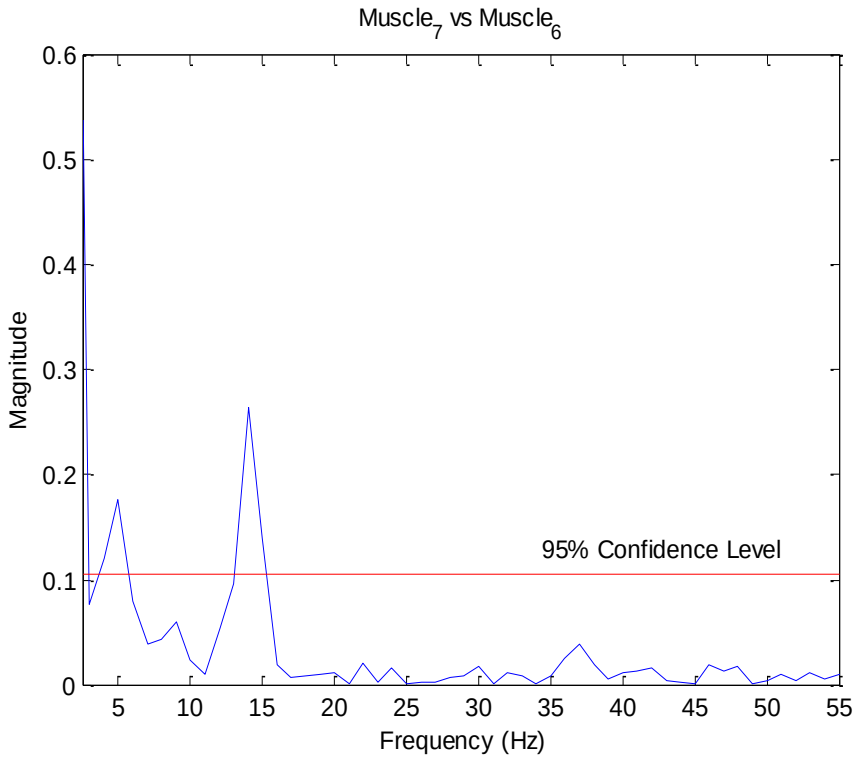

Figure 4.11 MD-PD Coherence from Target 2

Figure 4.11 takes a closer look at the coherence values for a specific muscle pair and target, in this case the relationship between the MD and PD muscles during Target 2 (0.4875, -0.8443, -0.2225). Significant activations occur at approximately 5 Hz and 15 Hz above the 95% confidence level, which correspond to common frequency ranges of motor activity within coherence analysis studies. Large spikes and incredibly high coherence values were also recorded between 200 and 600 Hz approximately. However, these values were disregarded, as literature research indicated that the range for motor unit firing was on a much smaller scale.

These results of the experimental data show significant coherence below 10 Hz, as well as peaks around 20 Hz. This suggests the occurrence of intermuscular coherence between certain groups at these lower frequencies. In addition to the frequency ranges of coherence being similar to recent publications, these values also potentially correspond to a common oscillatory input that leads to the motor unit recruitment, and therefore synergistic relationships between muscle groups.

To gain a better understanding of the overall relationships between muscle pairs, a table was created to show the strongest connections between each muscle. In Table 4.1, each muscle was paired against each other, with the pairs most commonly co-activated represented with "x" and a blank for those least co-activated during coherence analysis. This information was tabulated by visually inspecting each of the 432 graphs for peaks above the 95% confidence level and compiling the muscle pairs that most commonly displayed significant values.

	PECTclav	PD	MD	AD	TRIlat	TRIlong	BI
BRD		x					x
BI	x			x			
TRIlong		x		x	x		
TRIlat							
AD	x	x					
MD	x	x					
PD	x						

Table 4.1: Muscle co-activation patterns in coherence analysis

From Table 4.1, it can be observed that the most common relationships are BRD-PD, BRD-BI, BI-PECTclav, BI-AD, TRIlong-PD, TRIlong-AD, TRIlong-TRIlat, AD-PECTclav, AD-PD, MD-PECTclav, MD-PD, and PD-PECTclav. In order to evaluate the results of the coherence analysis against the synergistic pairs of the NMF analysis, another table was created for easier comparison.

	PECTclav	PD	MD	AD	TRIlat	TRIlong	BI
BRD	■						■
BI	■			■			
TRIlong		■	■		■		
TRIlat			■				
AD	■		■				
MD	■	■					
PD							

Table 4.2: Muscle co-activation patterns in NMF analysis

Table 4.2 shows muscle pairs found through the NMF approach and accounts for, on average, 95% of the variance in the dataset. The pairs discovered through the computational method include BRD-PECTclav, BRD-BI, BI-PECTclav, BI-AD, TRIlong-PD, TRIlong-MD, TRIlong-TRIlat, TRIlat-MD, AD-PECTclav, AD-MD, MD-PECTclav, and MD-PD. These relationships were tabulated in accordance to the completely NMF study, which also displayed muscle synergies in Figure 2.5. These tables show a number of commonalities and differences: for example, both have strong relationships between eight muscle pairs. However, the coherence analysis

also revealed a number of other strong relationships with regards to frequency that the NMF approach did not concur with, and vice versa.

4.2 Discussion

The purpose of this study was to reveal underlying synergistic pairs through coherence analysis of EMG muscles during an isometric force generation, as well as to investigate the commonalities between the correlational method of coherence vs the computational NMF approach.

4.2.1 Significant Results

The graphs of coherence between muscle pairs focused in on a range of 0 – 50 Hz, particularly due to the influence of the 0-20 Hz range, in which motor units and EMG oscillations are considered to be most active [6]. Additionally, previous studies have shown that co-contractions and large constant-torque loads during position holding have promoted variations in the 8-10 Hz range [8]. This could be considered relevant for this particular experiment, as the task involved position holding with a given force load. Based on previous studies, the actual frequency range in which coherence values appear to be significant strongly suggest a relationship between the given muscle pair, which in turn indicates the common oscillatory drive. As discussed earlier, the use of coherence analysis has the potential to reveal the recruitment of multiple motor units. The central nervous system plays an important role in the planning of movements to achieve them accurately and

efficiently through these motor units. I believe that the repeated occurrence of significant values in the 0-20 Hz range demonstrates a common drive in which the CNS can more effectively manage the varying degrees of freedom within motor control.

4.2.2 Comparison with NMF Approach

Through the NMF method, four primary synergies were revealed which accounted for, on average, 95% of the total variance of the EMG signals throughout the isometric force generation task. These four synergies (see Figure 2.5) was representative through the spatial, load, and position protocols. From these synergies, concurrent muscle groups were found to co-activate, which have been represented on Table 4.2. The synergies that are representative of the flexion and extension patterns from the NMF study share some muscle pairs with the relationships discovered through coherence analysis. Some significant relationships captured through both approaches include ones involving BRD, BI, PECTclav, MD, PD, TRIlong, and TRIlat. Each approach revealed twelve re-occurring muscle pairs. From these, eight were shared pairs and four pairs were different in each analysis. Some major differences include the lack of MD activation with any muscles below the shoulder (BRD, BI, TRIlong, TRIlat). These differences could be accounted for a variety of reasons – although the task for the coherence study replicated the same concept of the NMF study, the number of trials used in the NMF were both greater and more varied. The task for which the coherence analysis was performed can be viewed as a

reaching and holding task, which corresponds only to the spatial protocol task for the NMF study, which used 210 trials. The greater number of trials, as well as inclusion of the load and position protocols, could serve as a reason for differences within muscle co-activations. Additionally, both the number of subjects as well as the subjects themselves differed, although all subjects that participated in the study were healthy with no known problems. Although some muscle relationship differences were observed, I believe that the coherence analysis does in fact suggest the presence of strong muscle co-activations and synergies, particularly within the relationships that expressed similarities, therefore supporting the synergies revealed through the NMF study.

4.2.3 General Considerations

Muscle synergies can be regarded as a simplification of a complex and redundant mechanical system in charge of controlling movements, and their presence across varied tasks, specifically within the NMF approach, suggests the role that the CNS may play [13]. The supplemental evidence of the low range frequencies revealed through coherence analysis also supports the hypothesis of a common drive with multiple motor unit recruitment.

Some studies have shown that artifact signals can often occur during recording of EMGs through surface electrode during movement tasks, particularly with high levels of movement range and speed [17]. However, since the task involved a stationary gimbal that recorded the force, both movement and speed were not factors

in this study, thus reducing the potential for artifacts. Additionally, cross talk between EMG channels could affect the recordings and extraction of synergies. However, previous studies have shown that even after analysis on cross-talk affected muscles, the synergies that are revealed do not undergo any significant changes [13]. Muscle synergies may also include projections from the spinal interneuronal system to motorneuronal pools in the spinal cord. However, the intermediate zone neurons in the spinal cord correspond greater to muscle synergies than individual muscle activity (Hart – Neural basis for motor primitives).

Further studies will need to be performed to clarify the role of muscle synergies in regards to the CNS, as well as the muscle co-activations revealed through coherence analysis. This study can be continued by adding the load and position protocols for significant coherence values.

4.3 Implications

The objective of the study was to see if there were patterns between muscles during co-activation in this specific isometric force generation task. The muscle co-activation patterns that were then discovered may indicate of potential underlying neuronal activity. Specifically, this may suggest that the central nervous system uses these synergies in an interconnected and segmented fashion to have better control over movement and force control [13]. Since the possibilities for controlling muscles can be both incredibly redundant and complex, this approach of synergistic muscle activation seems likely.

From a clinical standpoint, the implications of further discovering muscle synergy and co-activation patterns can be extremely useful. Understanding the specific neuromuscular pathway from cortex to muscle fiber could potentially provide information in preventing or reversing neuromuscular diseases. Additionally, this information may be vital in the advancement of better designing orthopedic related products, such as prosthetics. The use of a smaller number of variables in order to address more degrees of freedom within the CNS may allow for simpler and more efficient neuro-prosthetics.

Chapter 5

Conclusion

Motor coordination plays an important role in an individual's daily life. Having a better understanding of motor control and movement patterns, controlled by the central nervous system, can be very beneficial in for the advancement of medical technology and assisting therapeutic treatments of neuromuscular diseases.

In this study, the synergistic relationships between muscles were observed from EMG signals during isometric force generation tasks involving spatial, load, and position protocols. The underlying muscle synergies were first revealed through a computational NMF approach, and then the spatial task was replicated to reveal any muscle co-activation pairs through coherence analysis.

It was shown that certain co-activation groups exist in accomplishing a given isometric force generation task when analyzed through coherence analysis, as shown in Table 4.1. These observed groups had eight common muscle pairs that resulted from both forms of analyses – potentially indicating a reoccurrence of muscle synergies or co-activations. The results indicate that the low frequency range of the co-activation pairs, similar to coherence ranges in previous studies, suggest a

common oscillatory drive for which motor unit recruitment is utilized as efficient mechanisms for the central nervous system in motor output.

It is hoped that this study provided much useful information in the way muscles are activated. These synergies suggest there is a task dependent recruitment when performing these force generating tasks, as well as a more modular approach by the CNS in tackling motor control.

Appendix A

Target 23 Results

BRD vs. All

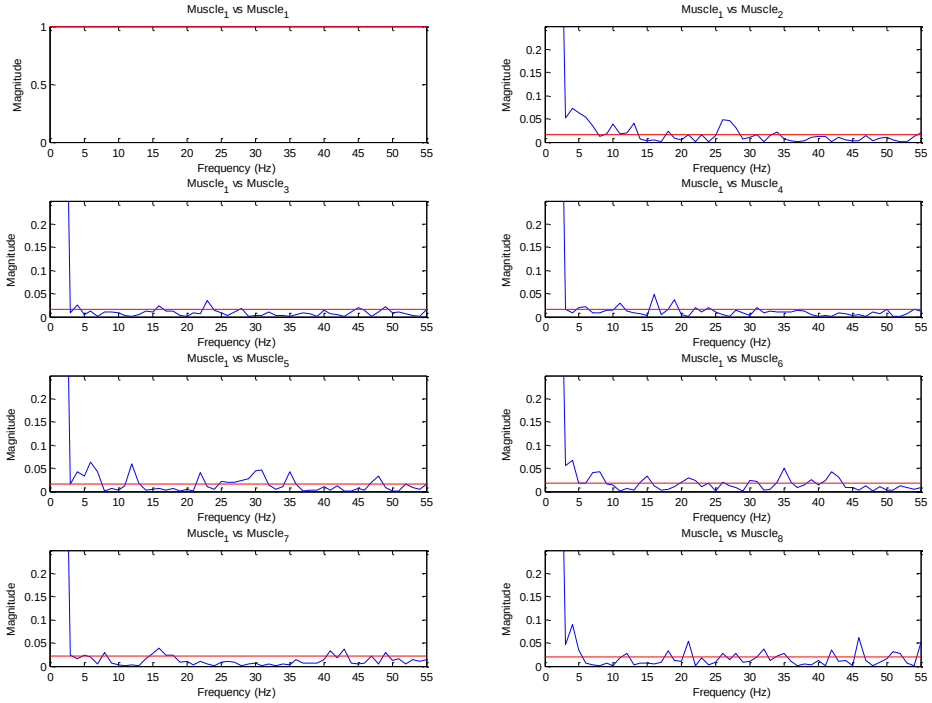

BI vs. All

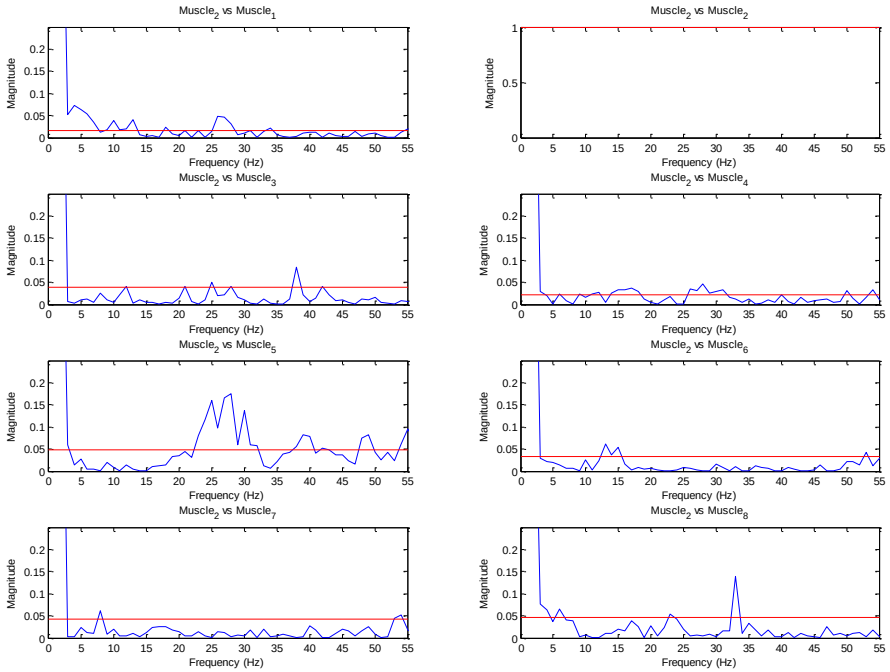

TRIlong vs. All

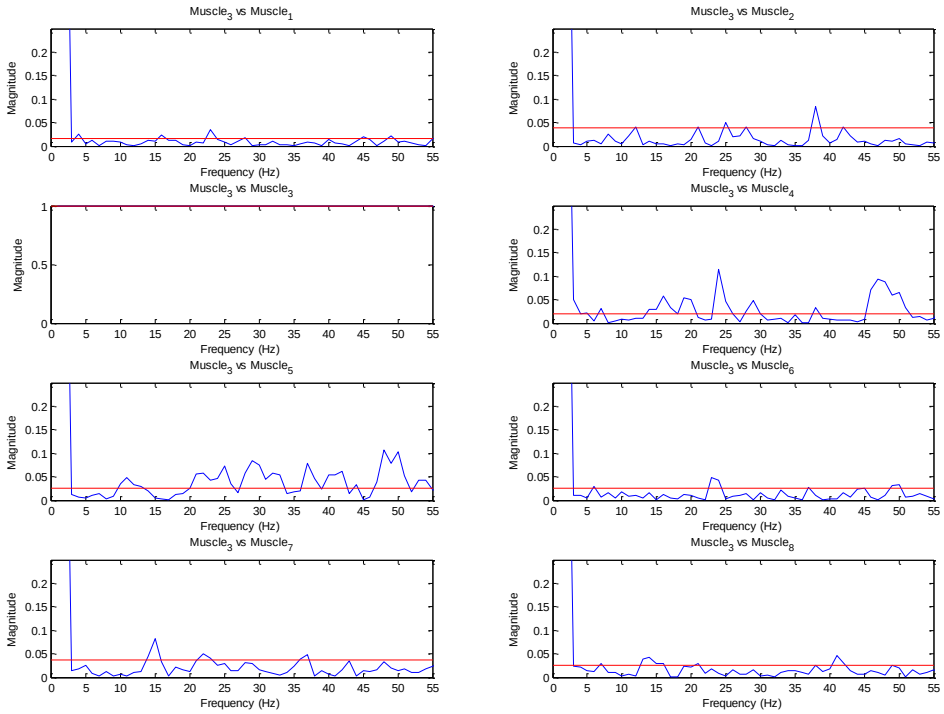

TRIlat vs. All

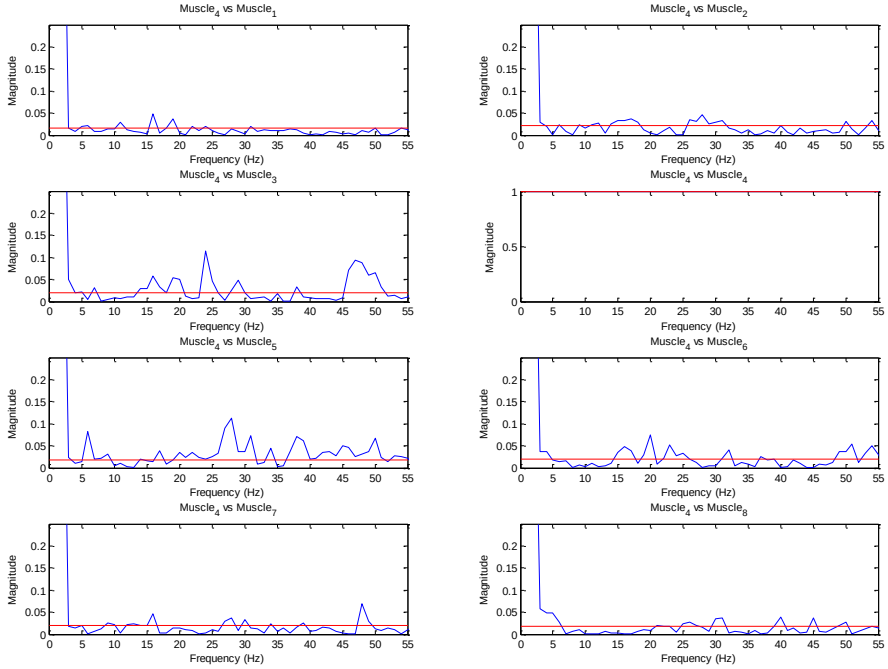

AD vs. All

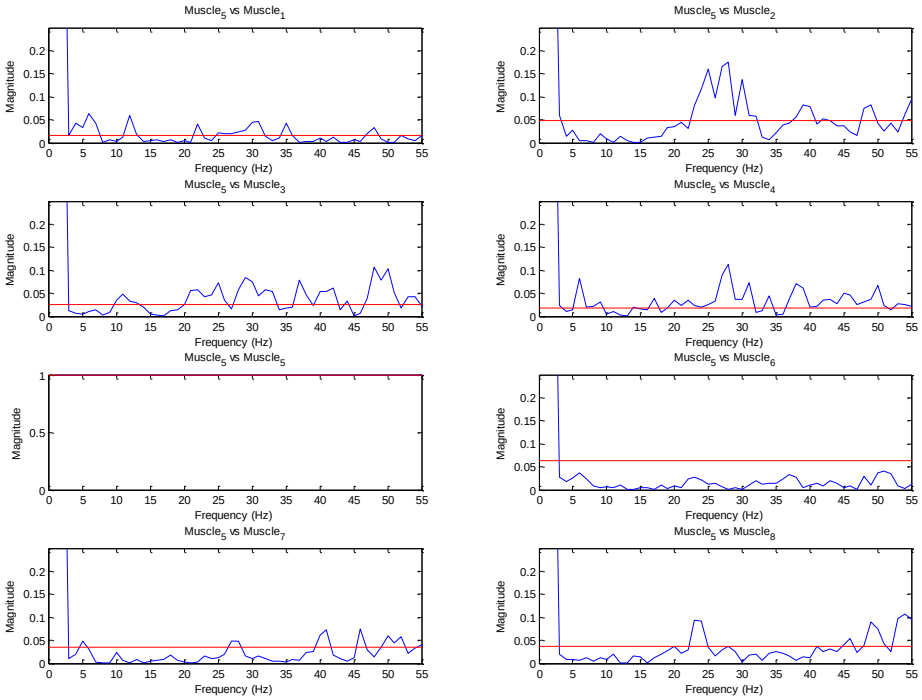

MD vs. All

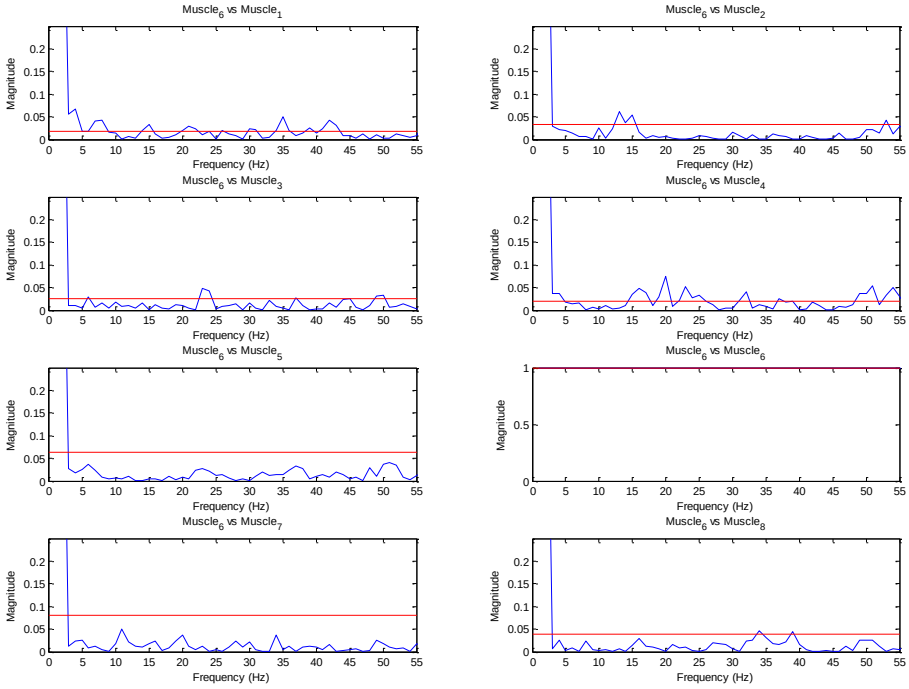

PD vs. All

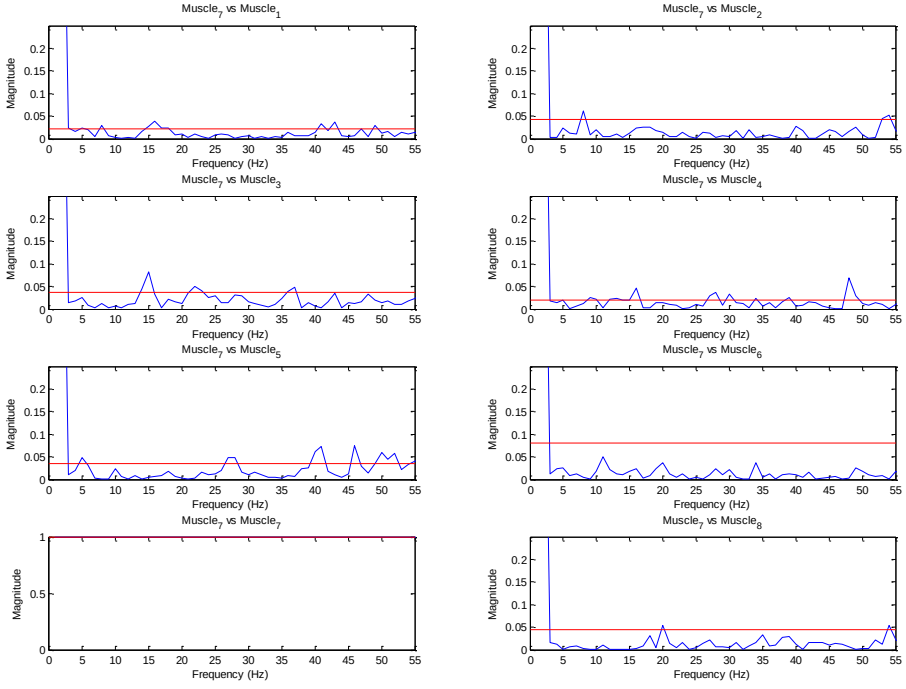

PECTclav vs. All

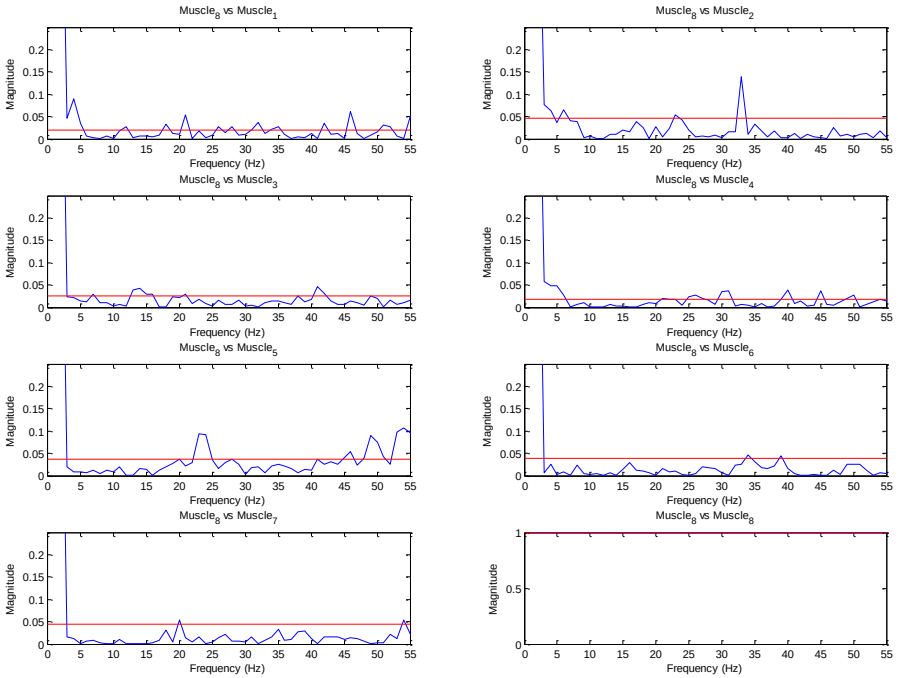
Muscle8 vs Muscle1
Muscle8 vs Muscle2
Muscle8 vs Muscle3
Muscle8 vs Muscle4
Muscle8 vs Muscle5
Muscle8 vs Muscle6
Muscle8 vs Muscle7
Muscle8 vs Muscle8
Magnitude
Frequency (Hz)

Appendix B

MATLAB Code

```
clc;
clear all;
close all;



%% Load Dataset


totaldat = daqread('EMGdata_013.daq', 'Channels', 1:8);
% Use totaldat only for the one continuous data file
data = totaldat(1:96000,:);


samp = 1920; %Sampling Frequency (Hz)


%% Trial by Trial Analysis


m=8;
channels=(0:m-1);
numofchan=length(channels);
finaldata = data(:,1:8);
```

```
name2 = cell(0,7);
subnum2 = (1:8);
cohere = cell(0,7);

refindex = 8; %Set channel as reference
refchannel = finaldata(:,refindex); %obtain entire
channel data set

for m=1:numofchan; %Run loop through dataset
    cohere{m} =
mscohere(finaldata(:,m),refchannel,hanning(samp),(samp/2
),samp);
end

coh_dat = cell2mat(cohere);

%% Peak Analysis, 95% Confidence Interval

r = 8;
t = 1.646; %t-value for one sided CI at 95%

for r=1:numofchan
```

```
    dat{r} = coh_dat(:,r);
    avg{r} = mean(dat{r});
    stdev{r} = std(dat{r});
    UB{r} = avg{r} + ((t*stdev{r})/(sqrt(961))); %upper
bound limit
end



figure(2)
for r=1:numofchan;
    subplot(4,2,r);
    plot(coh_dat(:,r));
    axis([0 55 0 0.25]);
    xlabel('Frequency (Hz)'); ylabel('Magnitude');
    title(strcat('Muscle_8 vs Muscle_',num2str(r)));
    line = refline(0,UB{r});
    set(line,'Color','r')
end
```

References

[1] - Agnieszka Kitlas Golińska, “Coherence function in biomedical signal processing: a short review of applications in Neurology, Cardiology and Gynecology” Studies in Logic, Grammar, and Rhetoric. 25 (38) 2011

[2] – Arbib, M., 1981. Perceptual structures and distributed motor control: Brooks, V.B. (Ed.), Handbook of Physiology, Section 2: The Nervous System, Vol. II, Motor Control, Part I. American Physiology Society, pp. 1449–1480.

[3] – Barkhaus, P. “EMG Evaluation of the Motor Unit - Electrophysiologic Biopsy”. Retrieved Oct. 15, 2012.

[4] – Biometrics. “Bagnoli Desktop EMG System”. Retrieved Oct. 15, 2012; http://biometricsmotion.intoto.nu/produkten.php?ms_id=307&Bewegingsanalyse/EMG/Delsys/Delsys_Bagnoli

[5] – Bizzi E, Cheung VCK, d'Avella A, Saltiel P, Tresch M (2008). Combining modules for movement. *Brain Res Reviews* 57:125-133

[6] - Boonstra, Breakspear. “Neural Mechanisms of Intermuscular Coherence: Implications for the Rectification of Surface Electromyography” *J Neurophysiol* 107:796-807, 2012

[7] – Cheung VCK, d'Avella A, Tresch MC, Bizzi E (2005.) Central and sensory contributions to the activation and organization of muscle synergies during natural motor behaviors. *J Neurosci* 25:6419-6434

[8] – Cram et al. “The History of Muscle Dysfunction and sEMG”. Journal of Applied Psychophysiology and Biofeedback. Retrieved Oct. 15, 2012

[9] - Danna-Dos Santos, Poston, Jesunathadas. “Influence of Fatigue on Hand Muscle Coordination and EMG-EMG Coherence During Three-Digit Grasping” *J Neurophysiol* 104: 3576–3587, 2010.

[10] – Dartnall T, Nordstrom M, Semmler G – “Motor Unit Synchronization Is Increased in Biceps Brachii After Exercise-Induced Damage to Elbow Flexor Muscles” *J Neurophysiol*. 2008 Feb;99(2):1008-19

[11] - Delagi EF, Perotto A. “Anatomical Guide for the Electromyographer”. Springfield, IL: Charles C. Thomas, 1980

[12] - Farmer et al. “Changes in EMG Coherence Between Long and Short Thumb Abductor Muscles During Human Development” *J Physiol* 579.2 (2007) pp 389–402: Figure 2C.

[13] – Grosse P, Edwards M, Tjissen MA, Schrag A, Lees AJ, Bhatia KP, Brown, P. “Patterns of EMG-EMG Coherence in Limb Dystonia”. *Mov Disord.* 2004 Jul; 19(7): 758-769

[14] - Halliday D.M., Rosenberg J.R., Amjad A.M., Breeze P., Conway B.A. & Farmer S.F. “A Framework For the Analysis of Mixed Time Series/Point Process Data - Theory and Application to the Study of Physiological Tremor, Single Motor Unit Discharges and Electromyograms”, *Progress in Biophysics and molecular Biology*, 64, 237-278, 1995.

[15] – Hermens HJ, Freriks B, Merletti R, Stegeman D, Blok J, Rau G, Disselhorst-Klug C, Hagg GG. “European Recommendations for Surface Electromyography, Results of the SENIAM Project.” *Signal Processing*. Netherlands: Roessingh Research and Development, 1999, p. 8-11

[16] – Kimball, J. “Kimball’s Biology Pages”. Retrieved Oct 15, 2012

[17] - Katarzyna Kisiel-Sajewicz et al. “Weakening of Synergist Muscle Coupling During Reaching Movement in Stroke Patients” *Neurorehabil Neural Repair* 2011, 25: p 359

[18] – Lee and Seung. “Learning the Parts of Objects by Non-Negative Matrix Factorization” *Nature* 401: 788-791, 21 October 1999

[19] - Mima, Toma, et al. “Coherence Between Cortical and Muscular Activities After Subcortical Stroke” *Stroke* 32: 2597-2601, 2001

[20] – Mima et al. “Force level modulates human cortical oscillatory activities.” Neuroscience Letters, Volume 275, Issue 2, 12 November 1999, Pages 77–80

[21] - Radoslav Bortel, Pavel Sovka, “EEG–EMG coherence enhancement” Signal Processing, Volume 86, Issue 7, July 2006, Pages 1737–175

[22] – Roh et al. “Robustness of Muscle Synergies Underlying Three-Dimensional Force Generation at the Hand in Healthy Humans” J Neurophysiol 107: 2123–2142, 2012

[23] - Rosenberg et al. “The Fourier Approach to the Identification of Functional Coupling Between Neuronal Spike Trains” *Pro 0. Biophys. molec. Biol.*, Vol. 53, pp. 1-31, 1989

[24] – Sandbrink, F. “Motor Unit Recruitment in EMG Definition of Motor Unit Recruitment and Overview”. Retrieved Oct. 15, 2012

[25] - Schoffelen JM, Oostenveld R, Fries P (2005). Neuronal coherence as a mechanism of effective corticospinal interaction. *Science* 308:111–113.

[26] – Tresch MC, Jarc A (2009) The case for and against muscle synergies. *Curr Opin Neurobiol* 19:1-7

[27] - Welch PD. **“**Use of Fast Fourier Transform for Estimation of Power Spectra–a Method Based on the Averaging Over Short Modified Periodograms.” *IEEE Trans Audio Electroacoustics* AU15: 196770–73.

[28] – “What is an EMG?” BME 366 Lab, SMPP – RIC. http://smpp.northwestern.edu/bmec66/weightlifting/emgback.html